ScientificScholar®
Knowledge is power
Publisher of Scientific Journals

www.clinicalimagingscience.org

Journal of Clinical Imaging Science

Technical Innovation *Cardiopulmonary Imaging*

Next-generation digital chest tomosynthesis

Christopher Gange[1], Jamie Ku[2], Babina Gosangi[1], Jianqiang Liu[2], Manat Maolinbay[2]

[1]Department of Radiology and Biomedical Imaging, Yale University, New Haven, Connecticut, [2]Product Development, Aixscan Inc., Sunnyvale, California, United States.

***Corresponding author:**
Christopher Gange,
Department of Radiology
and Biomedical Imaging,
Yale University, New Haven,
Connecticut, United States.

christopher.gange@yale.edu

Received: 04 January 2024
Accepted: 17 April 2024
Published: 26 June 2024

DOI
10.25259/JCIS_4_2024

Quick Response Code:

ABSTRACT

The objective of this study was to demonstrate the performance characteristics and potential utility of a novel tomosynthesis device as applied to imaging the chest, specifically relating to lung nodules. The imaging characteristics and quality of a novel digital tomosynthesis prototype system was assessed by scanning, a healthy volunteer, and an andromorphic lung phantom with different configurations of simulated pulmonary nodules. The adequacy of nodule detection on the phantoms was rated by chest radiologists using a standardized scale. Results from using this tomosynthesis device demonstrate in plane resolution of 16lp/cm, with estimated effective radiation doses of 90% less than low dose CT. Nodule detection was adequate across various anatomic locations on a phantom. These proof-of-concept tests showed this novel tomosynthesis device can detect lung nodules with low radiation dose to the patient. This technique has potential as an alternative to low dose chest CT for lung nodule screening and tracking.

Keywords: Medical imaging, Tomosynthesis, Chest radiography, Lung nodules

INTRODUCTION

Despite being around for over 100 years, chest X-ray remains one of the most frequently performed studies in radiology. While film and analog controls have been replaced with digital sensors, the basic procedure has remained constant throughout the years, due to the diagnostic utility of being able to "peek inside" the lungs, by passing an X-ray beam through the patient and measuring the amount of the beam that has passed through to assess the density of chest structures. The improved anatomic detail of cross-sectional imaging methods such as computed tomography (CT) has largely replaced chest X-ray for many indications since the 1990's, such as screening for and staging cancer. Large trials have shown that CT is superior to X-ray for the detection of lung nodules,[1] but CT has drawbacks, including a higher radiation dose to the patient and much higher capital costs for deployment. Despite these limitations and drawbacks, imaging volume for chest CT has continued to grow.[2] This volume growth has partly been checked by limited access, as lung imaging remains underutilized, especially for lung cancer screening and chronic disease detection.[3]

Chest tomosynthesis is a technique that evolved from geometric tomosynthesis which was first developed in the 1930's as an attempt to improve on two-dimensional (2D) imaging by moving the source in a motion that allowed for imaging in a single plane while blurring other overlying

structures. Tomosynthesis techniques were mostly replaced by CT, but tomosynthesis has recently gained interest as improvements in computer processing and digital sensors have made the technique more practical for clinical use. Modern tomosynthesis is an imaging technique that uses a shifting projection angle and algorithmic reconstructions to create multiple focused imaging planes with a fixed detector. By acquiring multiple slices, this scanning technique can provide three-dimensional (3D) data, which allows for better anatomic characterization then 2D techniques such as chest X-ray. The limited range of slices used in tomosynthesis results in less radiation dose to the patient compared to Chest CT.[4,5] The hardware requirements for tomosynthesis are also more limited compared with CT, and current X-ray systems have been modified to perform these exams.

Given the potential ability to improve the quality of chest X-ray imaging by providing additional 3D data without the need for expensive hardware or significantly increased radiation doses associated with CT, several vendors developed chest tomosynthesis systems and the Food and Drug Administration granted approval in 2006.[5] The current systems on the market that perform tomosynthesis are X-ray machines with modifications that allow for the 3D imaging technique. These machines use a single source and single detector and scan the chest through a limited set of angles in the craniocaudal dimension.[6]

Since approval led to wider availability, chest tomosynthesis has been tested for a wide variety of applications to identify appropriate clinical use and has been found to be better that chest X-ray for detecting pulmonary nodules[7-10] and useful for excluding unclear findings on chest X-ray that could require further work up.[11] Chest tomosynthesis has also shown utility in other applications such as cancer staging,[12] rating bronchiectasis in cystic fibrosis patients,[13] evaluating the lung hila in cases of suspected adenopathy,[14] evaluating pleural plaques in asbestos exposure cases,[15] excluding active tuberculosis,[16] evaluating for foreign bodies in the airways,[17] and evaluating for the presence of honeycombing in interstitial lung disease.[17] Studies comparing chest tomosynthesis to chest CT for detecting lung nodules have reported satisfactory results.[18,19] Despite the reported accuracy, several studies have reported limitations in chest tomosynthesis, including a lack of sensitivity for nodules in the lung apices and lung bases.[14,20]

This study introduces a system that is designed to address the limitations of chest tomosynthesis in currently approved systems using multiple X-ray sources and scanning along a transverse angle which moves from side to side of the patient. By creating custom equipment that is designed specifically for tomosynthesis instead of using modifications of standard X-ray equipment, there are fewer constraints on the hardware and imaging techniques that can be performed. This study will describe the imaging characteristics achieved by this novel device, show example images taken from a healthy volunteer, and demonstrate the ability to detect lung nodules using a phantom.

MATERIAL AND METHODS

System design

The tomosynthesis system tested in this report is referred as generation 2.5 (G2.5) and shown in Figure 1. It is a prototype system for clinical patient imaging. It uses 5 X-ray sources that move independently to capture a gantry span angle of 60°. A large, 86 × 43 cm flat panel detector with 15 frame per second rate is used for the current G2.5 system. A high-speed detector is being developed for future clinical systems, which will reduce the scan down to 2 s.

While tomosynthesis technique in general has wide applications in clinical radiology, this report is focused on thoracic imaging. The scan parameters and protocols used for the images in this study are detailed in Table 1. For lung imaging, adequate image quality can be achieved with 80 projections in 7 s scan time. However, further improvement of image quality can be achieved by increasing the projection to 120, which linearly increases the scan dose and scan time.

Radiation dose and safety tests

The radiation dose delivered by tomosynthesis systems is typically much lower than CT, even considering the low-dose

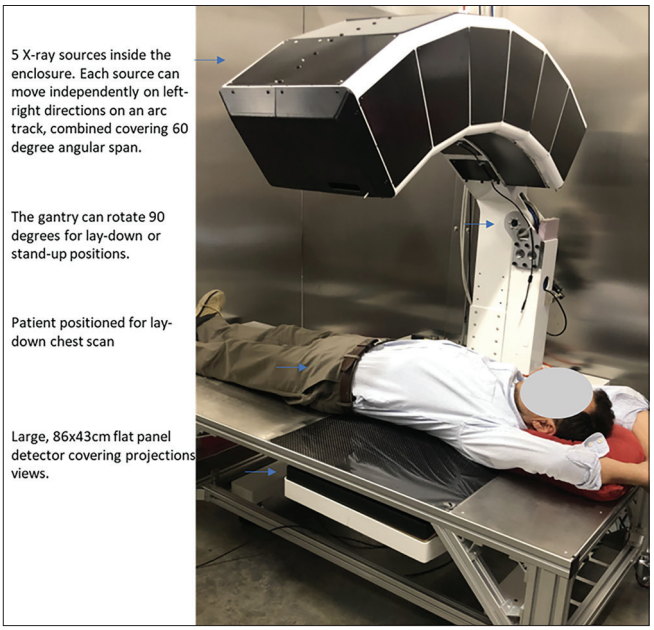

Figure 1: Photograph of AIxscan generation 2.5 (G2.5) tomosynthesis system. Feature descriptions are on the left and highlighted by blue arrows. The G2.5 is a prototype system for clinical patient imaging.

Table 1: G2.5 prototype system parameters used for chest tomosynthesis.

Scan type (Protocol)	Chest tomosynthesis
Projection span angle	60°
Scan direction	Left to right over the chest
Patient position on table	Supine with arms up
Number of projections*	40/80/120
Scan time*	3.6/7.2/10.8 s
Total scan mAs*	24/48/72 mAs
Tube added permanent filter	0.2 mm Cu
Tube kVp for small, medium, large patient	100, 110, 120 kVp
Reconstruction method	Filtered back projection
Total image processing and reconstruction time (Nvidia RTX3090 GPU)	50 s
Detector pixel size	0.308×0.308 mm^2
Detector pixel matrix	2816×1408
Reconstructed voxel size	0.28×0.28×0.84 mm^3
Reconstructed voxel matrix	1536×1536×384
Reconstructed volume size	43×43×28.4 cm^3
3D image format	DICOM

*The 3 scan times and the 3 mAs settings correspond to the 3 numbers of projection, respectively. DICOM: Digital imaging and communications in medicine, GPU: Graphics processing unit

protocols used with lung cancer screening CT. This reduction is possible because tomosynthesis requires fewer projections to create the image. Measured air KERMA and the estimated effective dose for a chest tomosynthesis protocol are shown in Table 2 for the 80 projections. The entrance air KERMA and the effective dose are 7 mGy and 0.185 mSv, respectively, for medium size patient with tomosynthesis.[21] For a given kVp, the dose linearly scales with the number of projections. For example, the dose for 40 projections is half of the dose for the 80 projections. As a comparison, the average effective dose for low dose CT (LDCT) is 1.5 mSv.[22]

The radiation beam quality was evaluated for this device. Excess low-energy soft X-rays can increase patient skin dose, while contributing little or no benefit for image quality. The soft X-rays are filtered out by adding 0.2 mm copper filters on each tube output window. X-ray beam quality test per IEC 60601-1-3 has been conducted and passes the requirement, as shown in Table 3. Tests for radiation leakage were also performed by assessing 5 points surrounding the unit.

Volunteer scan

Using the protocol listed in Table 1 with 110 kVp and 120 projections, an asymptomatic volunteer was consented and scanned for the purpose of visual observations and evaluations of the system performance to address the quality of scans for human imaging. The volunteer was a 60-year-old male weighing 80 kg, with a history of smoking but no current diagnosed lung disease, no history of malignancy, and no clinical symptoms.

The reconstructed volume matrix size is 1536 × 1536 × 384, where each image consists of 1530 × 1530 pixels in the coronal plane, and there are 384 coronal slices. The voxel cubic size is 0.28 mm × 0.28 mm × 0.84 mm, where 0.84 mm is the slice thickness. These scans were evaluated subjectively for quality but were not evaluated for clinical abnormalities.

Phantom nodule scans

Spatial resolution testing was performed using a line-pair phantom. The line pair phantom was scanned using the parameters listed in Table 1 with 120 projections.

Phantom testing was performed with the multipurpose Chest Phantom N1 "LUNGMAN" (Kyoto Kagaku, Kyoto, Japan). The phantom, as shown in Figure 2, is a life-size anatomical model of a human thorax and has been widely used in X-ray and CT imaging research. The soft tissue substitute material and synthetic bones have X-ray absorption rates similar to human tissues.

Imaging capability of the system was assessed using various simulated lung nodules inserted inside the phantom. The nodules are created by the phantom manufacturer to mimic the range of lung nodules found in practice. The size of nodules varies from 3 mm up to 20 mm, the nodule morphology includes spherical, mixed density (part-solid), and spiculated. The nodule density in Hounsfield Unit (HU) varies from +100HU (solid tumor type) to −800HU (pure groundglass opacity) type. Figure 3 shows the picture and reconstructed images of these nodules in the absence of any overlapping structures. Selected nodules were inserted inside the phantom for testing conspicuity.

To assess the conspicuity of small nodules, ten 5 mm acrylic balls (equivalent to +100HU nodules) were placed in varying locations in the phantom, with 5 on each side. The balls were held in place using plastic foam and Kapton tape inside the lung tree, as shown in Figure 4. The imaging was performed using the parameters in Table 1 with 120 projections. The images were rated by 2 practicing board certified chest radiologists (BG and CG) using an image quality scoring criteria shown in Table 4, adapted from criteria validated in CT.[23]

Another experiment to assess sensitivity was performed with nodules of varied sizes that were paired with a lower density, ground glass equivalent. Six spherical artificial nodules with size 8 mm, 5 mm and 3 mm, and density +100HU and −630HU were imaged. All six nodules were placed on the right side of the lung module. The imaging was performed using the parameters in Table 1 with 120 projections. These nodules were assessed using the criteria from Table 4 by a

Table 2: Typical dose for tomosynthesis using the chest protocol scan parameters listed for 80 projections.

Patient weight	Tube kVp Selection	Number of projections	Reference entrance air KERMA. (Ion chamber reading at chest-top position), in mGy	Entrance air kerma to effective dose conversion factor, mSv/mGy, based on reference	Estimated Effective dose in mSv
Small	100kVp	80	4.02	0.15	0.60
50–70 kg		120	6.03	0.15	0.90
Medium	110kVp	80	5.42	0.165	0.89
70–85 kg		120	8.13	0.165	1.34
Large	120kVp	80	7.0	0.185	1.30
85–95 kg		120	10.5	0.185	1.94

KERMA: Kinetic energy released per unit mass

Table 3: X-ray beam quality test results.

tube kVp	Aluminum filter thickness (mm)*	Exposure without Al filter (mR)	Exposure with Al filter (mR)	Measured attenuation	Maximum permissible attenuation (%)*	Beam quality
100	3.6	3.84	2.58	32.8	50	Pass
110	3.9	5.2	3.49	32.9	50	Pass
120	4.3	6.83	4.59	32.8	50	Pass

*IEC 60601-1-3 (IEC 2008), 3-Half value layers, Al: aluminum

Table 4: Scoring criteria used for nodule adequacy (adapted from).

0=Nodule not seen
1=Unacceptable quality (images do not allow diagnostic interpretation)
2=Limited quality (images are adequate only for limited clinical interpretation due to high noise and blur)
3=Adequate quality (images are just adequate for diagnostic interpretation)
4=Higher than needed quality (images are much better than needed for interpretation: images with little or no noise)

board certified radiologist (CG).

RESULTS

Visual grading of the line phantom shows the resolution to be 16 line-pair per centimeter in the imaged coronal plane. The line phantom results are shown in Figure 5.

Volunteer chest images

Representative images from volunteers are shown at different depths corresponding to anatomic landmarks, as shown in Figures 6-8.

Chest phantom nodule results

The scan time and the effective dose for phantom scan were 10.8 s and 0.14 mSv, respectively. A representative image through the mid chest of the phantom with nodules in place is shown in Figure 9. Example images of the nodules within the phantom

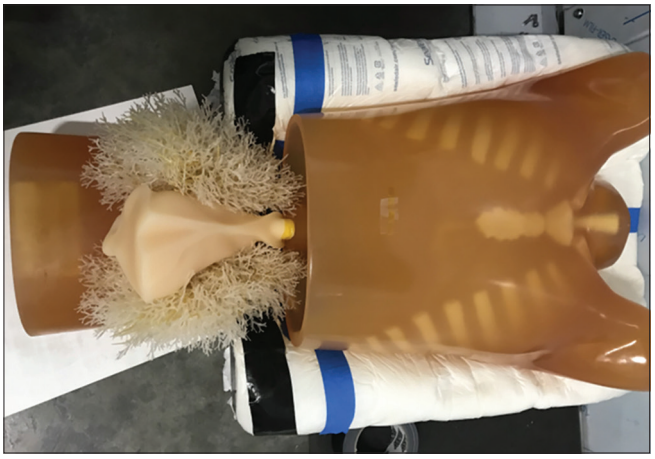

Figure 2: Chest Phantom N1 "LUNGMAN" (Kyoto Kagaku, Kyoto, Japan). Showing thorax, including lung/heart, and the upper abdomen.

are shown in Figures 10-12. The images of the nodules have been taken from the plane at which they were best defined.

The images shown in Figure 10a demonstrate results from the phantom with nodules of different attenuation. The displayed nodule was placed in the left-middle region of the lung. Both the ground glass and solid features of the nodule are scored as adequate (3). Figure 10b shows the irregular (intended as real tumor shaped) 3D ground glass density nodule. The nodule size is 1.5 cm, with density of −590HU. The example nodule was placed in the right-middle region of the lung. The nodule is visible on the scan and scored as adequate (3).

The image in Figure 11 shows examples of 12 mm diameter speculated and 8 mm diameter spherical nodules. Both

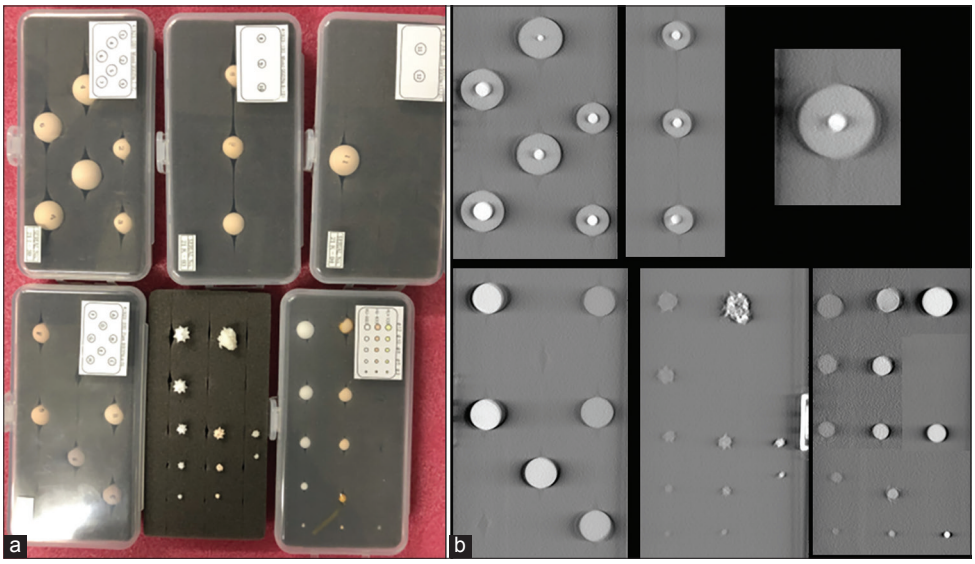

Figure 3: (a) Diverse set of simulated lung nodules are shown in the picture on the left. (b) images show the reconstructed tomosynthesis of the nodules. These nodules are scanned without any overlapping materials.

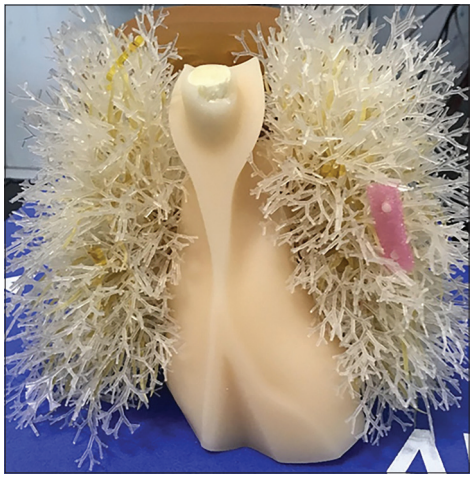

Figure 4: Ten 5 mm acrylic balls were placed in the lung tree, 5 balls on each side of the lung.

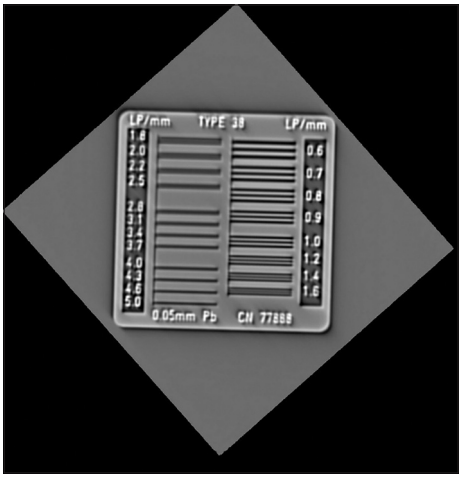

Figure 5: G2.5 System tomosynthesis spatial resolution measured with line-pair phantom, on the left.

nodules measure +100HU density. Both nodules were scored as higher than needed quality.

Each of the 5 mm nodules in the small nodule rating scan were graded as adequate or higher than needed. Examples of each nodule in plane are shown in Figure 13. The second experiment used pairs of balls that were matched by size but had different densities. The results of this test are shown in Figures 14 and 15.

DISCUSSION

The experiments and images reported in this study showed that this prototype tomosynthesis device is capable of detecting pulmonary nodules in a wide range of size and density in different anatomic regions. Other groups have reported that only 50% of nodules between 5 and 6 mm seen on CT are detected with currently available tomosynthesis units, and that pure ground glass nodules <10 mm were routinely missed.[24] Our results showed consistent detection for 5 mm solid nodules and adequate detection of all 8 mm ground glass nodules. The multiple source design and transverse scanning angle are intended to reduce artifacts in the tomosynthesis technique that limited nodule detection in other studies that used modified conventional radiography equipment. Our volunteer scan images showed limited

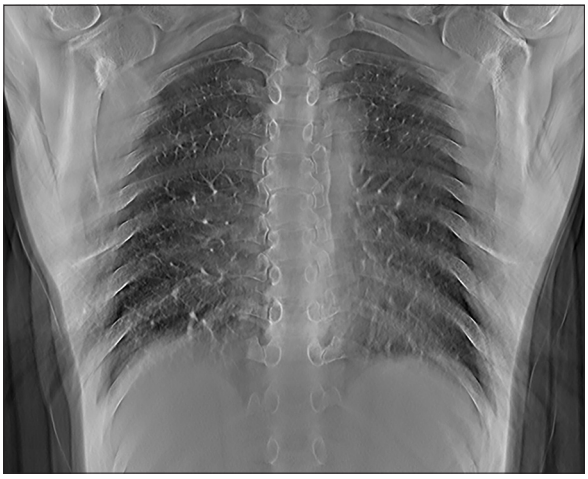

Figure 6: Representative tomosynthesis image through the posterior lungs. The depth level can be determined by the bony structures that are in plane, including the mid thoracic vertebral bodies. Note that the heart and mediastinal structures are out of plane and the retrocardiac left lung base is well visualized.

Figure 7: Representative tomosynthesis image through the mid chest. The depth level can be determined as the heart and airways are in plane. The airways are distinguishable from the other mediastinal structures and the central vascular structures with this technique.

Figure 8: Representative tomosynthesis image through the anterior chest. The ribs remain out of plane allowing evaluation of lung detail.

Figure 9: Representative midlung tomosynthesis slice of the chest phantom image with various nodules inserted inside the lung module. Nodules that are in plane are well defined, including a part solid nodule in the right mid lung and solid nodules in the left midlung.

motion artifact and image blur at the lung bases. This result will need to be validated in clinical trials with patients who have lung nodules or other disease using CT as a gold standard. Since the prototype was not yet installed in a medical clinic, this study was limited to only one individual and no concurrent chest CT images were available.

All images shown are in the coronal plane. Due to the limited angular coverage in tomosynthesis, in 3D reconstructed volume, only the planes parallel to the detector plane can produce high-resolution images. The spatial resolution in the axial and sagittal planes is poor. This will require an adjustment from the search pattern for looking for nodules compared to CT, where most radiologists focus on the axial image set. Flat panel detector based tomosynthesis has superior spatial resolution in the imaging plane however, compared to CT. This is because the flat panel detector pixel size (0.1–0.3 mm) is much smaller the CT detector pixel size (0.8–1.2 mm). This is demonstrated by the line pair resolution of 16 lp/cm for the tomosynthesis unit, compared to a typical CT resolution of 7 lp/cm.[25]

Sensitivity for clinical findings depends on whether superior in-plane resolution compensates for other artifacts inherent in tomosynthesis technique. The prototype used in this study was designed to minimize artifacts to improve the quality of the images, with the goal to improve detection of nodules

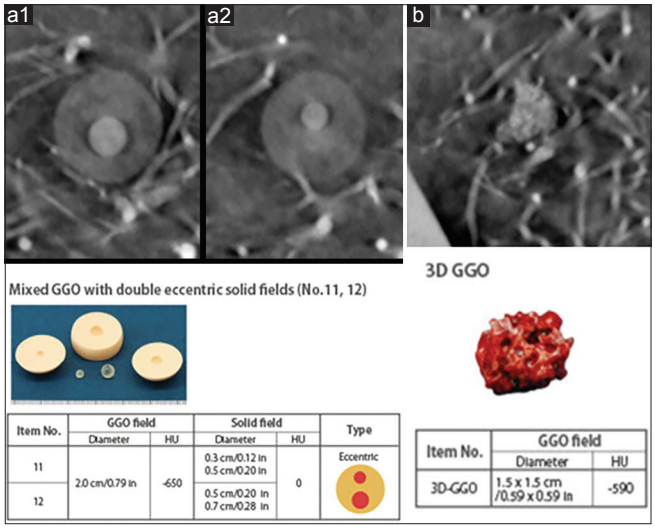

Figure 10: (a1 and a2) Demonstrate in-plane images of part solid pulmonary nodules including a Groundglass opacities (GGO) component of −650 Hounsfield Unit (HU) and a solid component measuring 0 HU. The size of the solid components in (a1 and a2) are 0.7 cm and 0.5 cm, respectively. The photograph of the nodule and technical specifications are shown below. (b) Demonstrates in plane tomosynthesis imaging of a pure ground glass nodule with picture and specifications below.

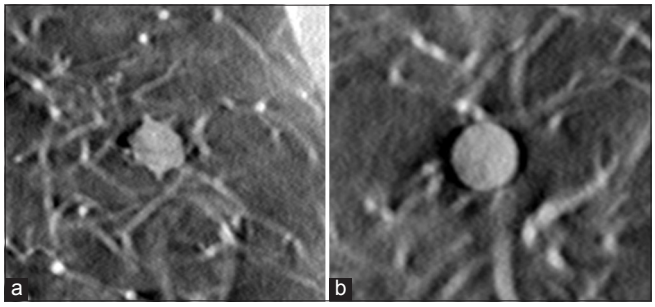

Figure 11: (a) In-plane tomosynthesis image of a 12 mm speculated nodule with +100 Hounsfield Unit (HU) density, placed at right-middle region of the lung. (b) In-plane tomosynthesis image of an 8mm spherical nodule with +100HU, placed at upper-right region of the lung.

and other findings to the level where the system can compete with CT to answer clinical questions. This design is intended to improve the quality of tomosynthesis imaging in several ways. First, the device is designed to complete the scan in less time which limits the effects of motion artifact and reduces the amount of time a patient needs to hold their breath. If quality is being actively monitored, lower breath hold times should allow for fewer repeat studies. Current commercial systems have a minimum time of 10 s but this prototype system was able to scan in a range of 2–6 s. This decreased scan time is achieved by having multiple X-ray sources, as opposed to the single source that is present on a device designed to take standard radiographs. The prototype design

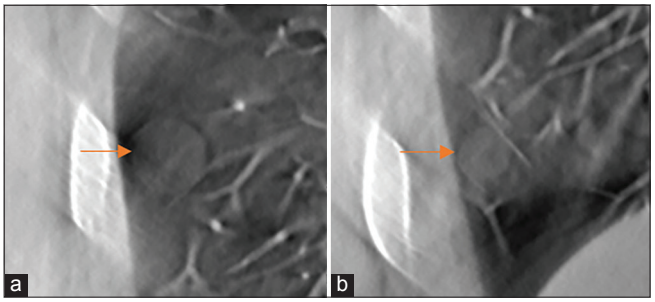

Figure 12: Spherical nodules with −800 Hounsfield Unit density (red arrows). The nodule diameters are (a) 12 mm and (b) 8 mm.

also achieves better resolution in the Z-axis by increasing the amount of degrees of the angular span. The G2.5 system has a maximum span of 60° while current available systems have a maximum of 40°. The increased angle can be achieved due to the change in axis of movement of the X-ray projector as transverse movement is not limited by patient anatomy.

This study was intended to show the image performance characteristics using a phantom. The nodule detection results will need to be replicated across the range of nodule sizes in human subjects and compared to the current gold standard of CT. Non-inferiority studies comparing the modalities will be needed before clinicians and patients trust a new modality for applications such as cancer staging. Lowered radiation dose compared to CT may help convince patients and some clinicians, but it is not clear that the reduction in dose is clinically significant, and CT radiation doses continue to improve. Careful testing of radiation doses will be necessary in a patient population that mimics the heterogeneity of the public, to ensure that chest tomosynthesis doses do not significantly increase in larger patients, and to ensure that the image characteristics are not significantly degraded in obese patients. If the reduction in effective dose for this device holds up in clinical trials, it could represent a decrease in dose of almost 90% compared to CT scanning, which has an average effective dose of 1.4 mSv for low-dose chest CT studies.[26] Even if the dose reduction does not have clearly definable risk reduction benefit, the principle of as low as reasonably achievable will favor tomosynthesis if is shown to be as accurate for a given clinical indication as CT.

Like any imaging modality, the scanner used in this study also introduces artifacts. On the left side of some of the volunteer images, there are line type and ripple type artifacts. These artifacts are caused by high lag ("ghosting") of the flat panel detector. Image lag is the residual signal from the previous exposed image frame. Further development of low lag, high-speed detectors will address these artifacts.

The prototype used in this study differs from other systems on the market in that it is a standalone device, not part of a package that includes a traditional X-ray machine.

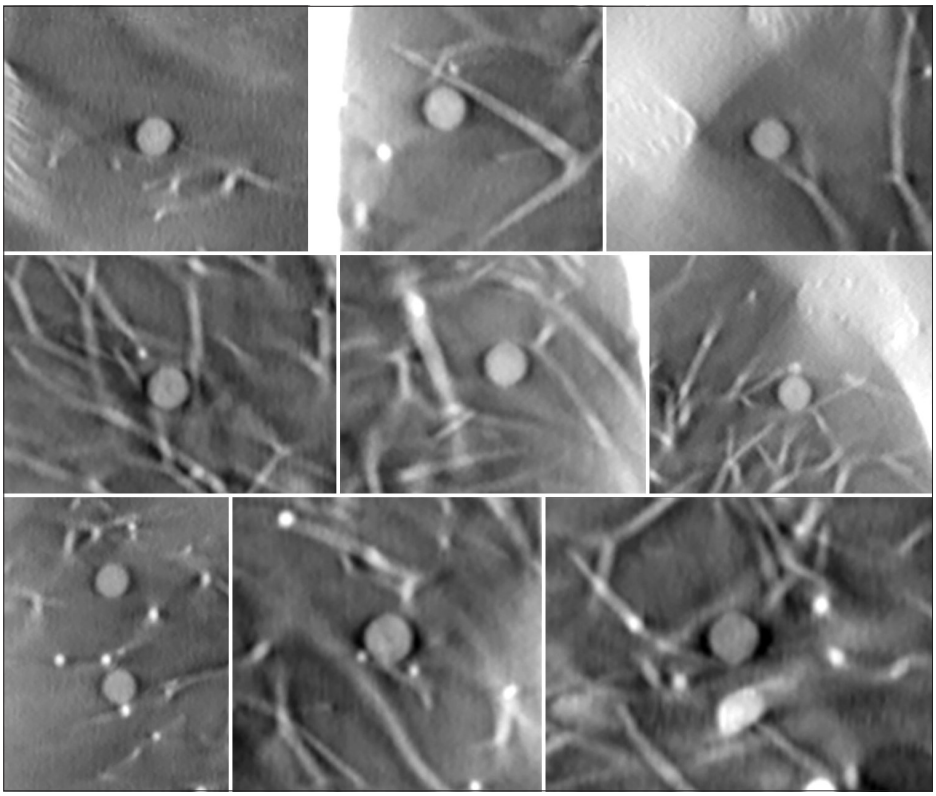

Figure 13: In-plane tomosynthesis images of the ten 5 mm acrylic balls (equivalent to +100 Hounsfield Unit nodules). Visibility is maintained at different anatomic locations.

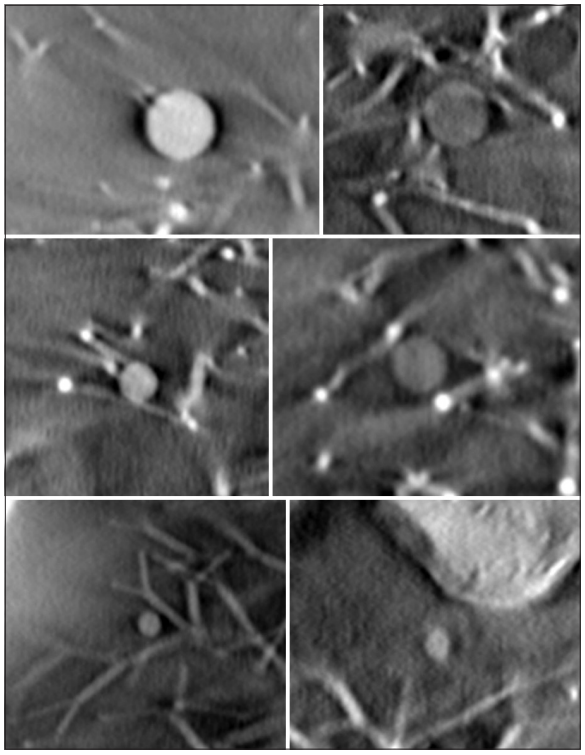

Figure 14: Cropped images of six spherical artificial nodules. Size of 8 mm, 5 mm, and 3 mm and density of +100 Hounsfield Unit (HU) and −630HU is indicated.

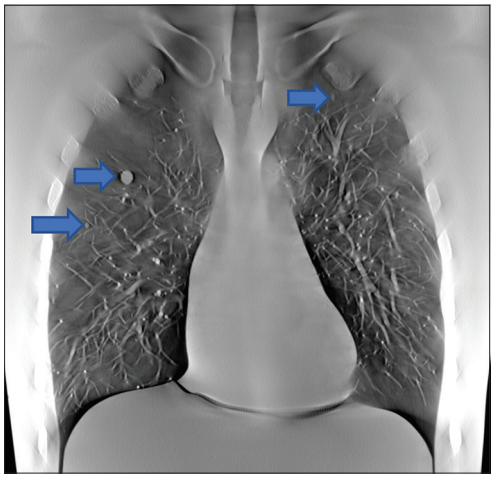

Figure 15: The image shows the full-size slice, where the three of the six nodules were shown by blue arrows.

Changing the design of tomosynthesis systems to address imaging shortcomings has financial considerations as well. A standalone device makes the system a bigger investment compared to retrofitting standard radiography machines, but the tomosynthesis unit remains much cheaper than a CT scanner and does not require custom electrical equipment such as transformers.

Despite a higher cost than chest X-ray, improved chest tomosynthesis systems could fill a need in diagnosis and managing chronic disease. By lowering the capital cost to deploy this system compared to CT, a wider number of clinics could potentially install this equipment, which could increase access to important but underused services such as lung cancer screening, which suffers from a lack of access to facilities, especially in rural areas where low volumes limit CT capacity.[3] If larger trials show that improved chest tomosynthesis systems approach the sensitivity of CT for common indications such as following pulmonary nodules, repeat staging of cancer, or following chronic lung disease such as pulmonary fibrosis, a wider variety of clinics would be able to offer these services due to the reduced capital requirements for deployment and lack of incumbent certificate of need constraints. Billing codes will have to be created that match the interpretation effort and cost of the new system. While the hardware costs less than CT, the interpretation effort will have to be accessed and fairly compensated to achieve widespread uptake by radiology practices.

An important indication for chest tomosynthesis is as an adjunct to chest X-ray, to reduce the need for further work up. The ability to clear patients with questionable findings on X-ray without further work-up (a chest CT or a subsequent repeat X-ray) is a reported use of built in tomosynthesis scanners that in theory could save health-care dollars, as studies have shown that most lesions seen on chest X-ray are pseudolesions.[11] This application of tomosynthesis will require more confidence by radiologists in interpreting these scans, and better reimbursement for the procedure before it is more widely practiced.

CONCLUSION

This study demonstrates the imaging characteristics for a new generation of tomosynthesis prototype device and how it applies to lung imaging. As with other tomosynthesis systems, the in-plane resolution is superior to Chest CT, with a lower radiation dose to the patient. Changing the axis of movement for the X-ray projector attempts to address the shortcomings of systems where the tomosynthesis is performed as an add on to standard radiography equipment. This study demonstrates the ability to detect a range of pulmonary nodules with this approach using a phantom. If further clinical testing validates this approach, than the advantages of lower cost and radiation dose may drive wider use of chest tomosynthesis.

Acknowledgments

The authors thank Linbo Yang for construction of the multiple X-ray sources.

Ethical approval

The Institutional Review Board approval is not required.

Declaration of patient consent

The authors certify that they have obtained all appropriate patient consent.

Financial support and sponsorship

This work was supported by AIxscan, who develops the device tested.

Conflicts of interest

This work was supported by AIxscan, who develops the device tested. Dr's Maolinbay, Liu, and Ku are employees of this company. Dr. Gange has a small ownership interest and acts as a medical adviser to AIxscan. Dr. Gange also reports research consulting for Bayer and Brainomx. Dr. Gosangi has no disclosures.

Use of artificial intelligence (AI)-assisted technology for manuscript preparation

The authors confirm that there was no use of artificial intelligence (AI)-assisted technology for assisting in the writing or editing of the manuscript and no images were manipulated using AI.

REFERENCES

1. National Lung Screening Trial Research Team, Aberle DR, Adams AM, Berg CD, Black WC, Clapp JD, *et al*. Reduced lung-cancer mortality with low-dose computed tomographic screening. N Engl J Med 2011;365:395-409.
2. Rosman DA, Duszak R Jr., Wang W, Hughes DR, Rosenkrantz AB. Changing utilization of noninvasive diagnostic imaging over 2 decades: An examination family-focused analysis of medicare claims using the neiman imaging types of service categorization system. AJR Am J Roentgenol 2018;210:364-8.
3. Kale MS, Wisnivesky J, Taioli E, Liu B. The landscape of US lung cancer screening services. Chest 2019;155:900-7.
4. Dobbins JT 3rd, Godfrey DJ. Digital X-ray tomosynthesis: Current state of the art and clinical potential. Phys Med Biol 2003;48:R65-106.
5. Dobbins JT 3rd. Tomosynthesis imaging: At a translational crossroads. Med Phys 2009;36:1956-67.
6. Dobbins JT 3rd, McAdams HP. Chest tomosynthesis: Technical principles and clinical update. Eur J Radiol 2009;72:244-51.
7. James TD, McAdams HP, Song JW, Li CM, Godfrey DJ, DeLong DM, *et al*. Digital tomosynthesis of the chest for lung nodule detection: Interim sensitivity results from an ongoing NIH-sponsored trial. Med Phys 2008;35:2554-7.
8. Dobbins JT 3rd, McAdams HP, Sabol JM, Chakraborty DP,

Kazerooni EA, Reddy GP, *et al*. Multi-institutional evaluation of digital tomosynthesis, dual-energy radiography, and conventional chest radiography for the detection and management of pulmonary nodules. Radiology 2017;282:236-50.
9. Kim JH, Lee KH, Kim KT, Kim HJ, Ahn HS, Kim YJ, *et al*. Comparison of digital tomosynthesis and chest radiography for the detection of pulmonary nodules: Systematic review and meta-analysis. Br J Radiol 2016;89:20160421.
10. Langer SG, Graner BD, Schueler BA, Fetterly KA, Kofler JM, Mandrekar JN, *et al*. Sensitivity of thoracic digital tomosynthesis (DTS) for the identification of lung nodules. J Digit Imaging 2016;29:141-7.
11. Quaia E, Baratella E, Cernic S, Lorusso A, Casagrande F, Cioffi V, *et al*. Analysis of the impact of digital tomosynthesis on the radiological investigation of patients with suspected pulmonary lesions on chest radiography. Eur Radiol 2012;22:1912-22.
12. Lee KH, Goo JM, Lee SM, Park CM, Bahn YE, Kim H, *et al*. Digital tomosynthesis for evaluating metastatic lung nodules: Nodule visibility, learning curves, and reading times. Korean J Radiol 2015;16:430-9.
13. Meltzer C, Gilljam M, Vikgren J, Norrlund RR, Vult von Steyern K, Båth M, *et al*. Quantification of pulmonary pathology in cystic fibrosis-comparison between digital chest tomosynthesis and computed tomography. Radiat Prot Dosimetry 2021;195:434-42.
14. Kim EY, Bista AB, Kim T, Park SY, Park KJ, Kang DK, *et al*. The advantage of digital tomosynthesis for pulmonary nodule detection concerning influence of nodule location and size: A phantom study. Clin Radiol 2017;72:796.e1-8.
15. Lee G, Jeong YJ, Kim KI, Song JW, Kang DM, Kim YD, *et al*. Comparison of chest digital tomosynthesis and chest radiography for detection of asbestos-related pleuropulmonary disease. Clin Radiol 2013;68:376-82.
16. Kim EY, Chung MJ, Lee HY, Koh WJ, Jung HN, Lee KS. Pulmonary mycobacterial disease: Diagnostic performance of low-dose digital tomosynthesis as compared with chest radiography. Radiology 2010;257:269-77.
17. Chou SH, Kicska GA, Pipavath SN, Reddy GP. Digital tomosynthesis of the chest: Current and emerging applications. Radiographics 2014;34:359-72.
18. Bertolaccini L, Viti A, Tavella C, Priotto R, Ghirardo D, Grosso M, *et al*. Lung cancer detection with digital chest tomosynthesis: First round results from the SOS observational study. Ann Transl Med 2015;3:67.
19. Zhao F, Zeng Y, Peng G, Yu R, Peng S, Tan H, *et al*. Experimental study of detection of nodules showing ground-glass opacity and radiation dose by using anthropomorphic chest phantom: Digital tomosynthesis and multidetector CT. J Comput Assist Tomogr 2012;36:523-7.
20. Lee KS, Chung MJ. Limitations of detecting small solid lung nodules by using digital chest tomosynthesis. Radiology 2018;287:1028-9.
21. Tungkum S, Suwanpradit P, Vidhyarkorn S, Siripongsakun S, Oonsiri S, Rakvongthai Y, *et al*. Determination of radiation dose and low-dose protocol for digital chest tomosynthesis using radiophotoluminescent (RPL) glass dosimeters. Phys Med 2020;73:13-21.
22. National Lung Screening Trial Research Team, Aberle DR, Berg CD, Black WC, Church TR, Fagerstrom RM, *et al*. The National Lung Screening trial: Overview and study design. Radiology 2011;258:243-53.
23. Padole AM, Sagar P, Westra SJ, Lim R, Nimkin K, Kalra MK, *et al*. Development and validation of image quality scoring criteria (IQSC) for pediatric CT: A preliminary study. Insights Imaging 2019;10:95.
24. Baratella E, Bozzato AM, Marrocchio C, Natali C, Di Giusto A, Quaia E, *et al*. Digital tomosynthesis and ground glass nodules: Optimization of acquisition protocol. A phantom study. Radiography (Lond) 2021;27:574-80.
25. Huda W, Abrahams RB. X-ray-based medical imaging and resolution. AJR Am J Roentgenol 2015;204:W393-7.
26. Larke FJ, Kruger RL, Cagnon CH, Flynn MJ, McNitt-Gray MM, Wu X, *et al*. Estimated radiation dose associated with low-dose chest CT of average-size participants in the National Lung Screening Trial. AJR Am J Roentgenol 2011;197:1165-9.

How to cite this article: Gange C, Ku J, Gosangi B, Liu J, Maolinbay M. Next-generation digital chest tomosynthesis. J Clin Imaging Sci. 2024;14:22. doi: 10.25259/JCIS_4_2024